J. Phys. B: At. Mol. Opt. Phys. 26 (1993) 2137–2151. Printed in the UK

Electron capture by doubly charged ions from laser-excited alkali atoms: I. He^{2+}–$Na^*(3p)$ collisions

M Gieler†, F Aumayr†, J Schweinzer†‖, W Koppensteiner†, W Husinsky†, H P Winter†, K Lozhkin‡ and J P Hansen§

† Institut für Allgemeine Physik, Technische Universität Wien, Wiedner Hauptstrasse 8–10, A-1040 Wien, Austria

‡ A F Ioffe Physical-Technical Institute, Politehnichenskaya 26, St Petersburg 194021, Russia

§ Fysisk Institutt, Allegaten 55, N-5000 Bergen, Norway

Received 7 December 1992, in final form 8 April 1993

Abstract. State-selective single electron capture in slow (0.5–3 keV amu^{-1}) collisions of He^{2+} with laser-excited $Na^*(3p)$ atoms has been studied by means of translational energy spectroscopy and the results compared with 64-state atomic orbital (AO) close coupling calculations, considering cross sections for electron capture into $He^+(n = 3, 4, 5)$ final states for different impact energies. In addition, alignment effects have been studied by controlling the polarization of the exciting laser light.

The experimentally observed dependence on $Na^*(3p\Sigma)$ and $Na^*(3p\Pi)$ initial state preparation is quantitatively reproduced by the AO calculations.

1. Introduction

The study of initial or final alignment of electronic charge cloud distributions in ion–atom collisions provides the possibility to investigate the quantum dynamics of electronic transitions at a fundamental level. Experiments dedicated to this purpose using excited atoms with well defined alignment and orientation of their initial magnetic substates provide a sensitive test of advanced atomic collision theories. Optical pumping with polarized laser light permitting the preparation of such well defined initial targets, during the last two decades led to a more detailed insight into the dynamics of inelastic collision processes (see e.g. Hertel and Stoll 1978, Campbell *et al* 1988).

First electron scattering experiments with laser excited Na by Hertel and Stoll (1974, 1978) have been followed by extensive studies on the $Na^+ + Na^*(3p)$ collision system (Bähring *et al* 1983, Witte *et al* 1987). Oriented Na and K atomic orbitals have been used as targets for scattering experiments at thermal energies by Düren and Hasselbrink (1986). Alignment effects of higher order have been observed in sophisticated experiments using two or even three lasers, in order to prepare target atoms in highly excited Na(4d) (Campbell *et al* 1990) and Ca(4s4f) (Driessen *et al* 1991) states, or for $Na^*(3p) + Na^*(3p)$ collisions (Meijer *et al* 1987).

At somewhat higher collision energies (50 eV–10 keV), single electron capture (SEC) by protons from excited $Na^*(3p)$ has become a prototype reaction for such studies, because of its particular simplicity (Royer *et al* 1988, Finck *et al* 1988, Gieler *et al* 1991). Effects of initial orbital alignment could be experimentally demonstrated (Dowek *et al* 1990), and

‖ Present address: Max Planck Institut für Plasmaphysik, D-8046 Garching, Federal Republic of Germany.

0953-4075/93/142137+15$07.50

a strong enhancement in the production of $H(n = 2)$ final states from excited $Na^*(3p)$ as compared to Na(3s), and consequently in L_α emission was found by Royer *et al* (1988), Finck *et al* (1988) and Gieler *et al* (1991), in good agreement with theoretical predictions (Allan *et al* 1986). Recently, orientation effects in $H^+ + Na^*(3p)$ collisions have been investigated by Houver *et al* (1992). Their measurements were found to be in perfect agreement with the calculations of Dubois *et al* (1993). Recent experiments by Richter *et al* (1993) and calculations by Dubois *et al* (1993) show that quantum interference effects are dominating features in $H^+ + Na^*(3p)$ collisions, i.e. a simple relation between trajectories in the impact parameter calculation cannot be directly related to the quantum scattering amplitude. This becomes most obvious for excitation processes at intermediate energies, where the final state orientation vanishes (Hansen *et al* 1992), in sharp contrast to the impact-parameter-dependent right-hand collision orientation parameter which is negative.

In charge exchange processes involving multicharged ions, however, the Coulomb repulsion dominates, thus providing a cleaner picture for understanding reaction dynamics in terms of left-right passages leading to orientation and alignment phenomena (Roncin *et al* 1990, Hansen *et al* 1990). The present experiments on capture to doubly charged ions—and possibly future differential measurements—can give insight to reaction dynamics for capture from laser-excited $Na^*(3p)$ when the trajectory interpretation is more valid.

The first experimental studies on collisions of multicharged ions colliding with laser-excited Na atoms have been made by Aumayr *et al* (1991) who found drastic changes in the final state distribution of captured electrons as compared to collisions with the ground state target atoms.

In this paper we describe the experimental procedure of such studies in more detail and report on investigations of electron capture in He^{2+}–$Na^*(3p)$ collisions (impact energy range 0.5–3 keV amu^{-1}), where the initial orbital alignment of the target atoms has been controlled via polarization of the exciting laser light. First results (Aumayr *et al* 1992) showed a pronounced polarization-dependence of charge transfer into final $He^+(n = 3, 4)$ states, in agreement with a 39-state AO calculation.

Our calculations have now been extended to 64 AO states, to account for all possibly relevant electron capture channels as apparent from our experiments.

This paper is the first part of a group of publications concerning combined experimental and theoretical studies of electron capture in collisions of doubly charged ions with laser-excited alkali atoms. In a forthcoming paper (II) we will present similar investigations on $He^{2+} + Li^*(2p)$ collisions, and III will be devoted to Ne^{2+}/Ar^{2+}–$Na^*(3p)$ collisions.

2. Experiment

2.1. *Experimental set-up*

For inelastic ion scattering near the forward direction the kinetic energy change of the projectile becomes approximately equal to the involved inelastic reaction energy defect ΔE, which fact permits a direct determination of the related inelastic reaction channels. A translational energy spectrometer (cf figure 1(*a*)) described in detail by Aumayr *et al* (1989) has been used for studying the electron capture reaction channels

$$He^{2+} + Na(3s), Na^*(3p) \rightarrow He^+(n) + Na^+ + \Delta E \qquad (1)$$

by virtue of their corresponding energy defects (cf figure 2).

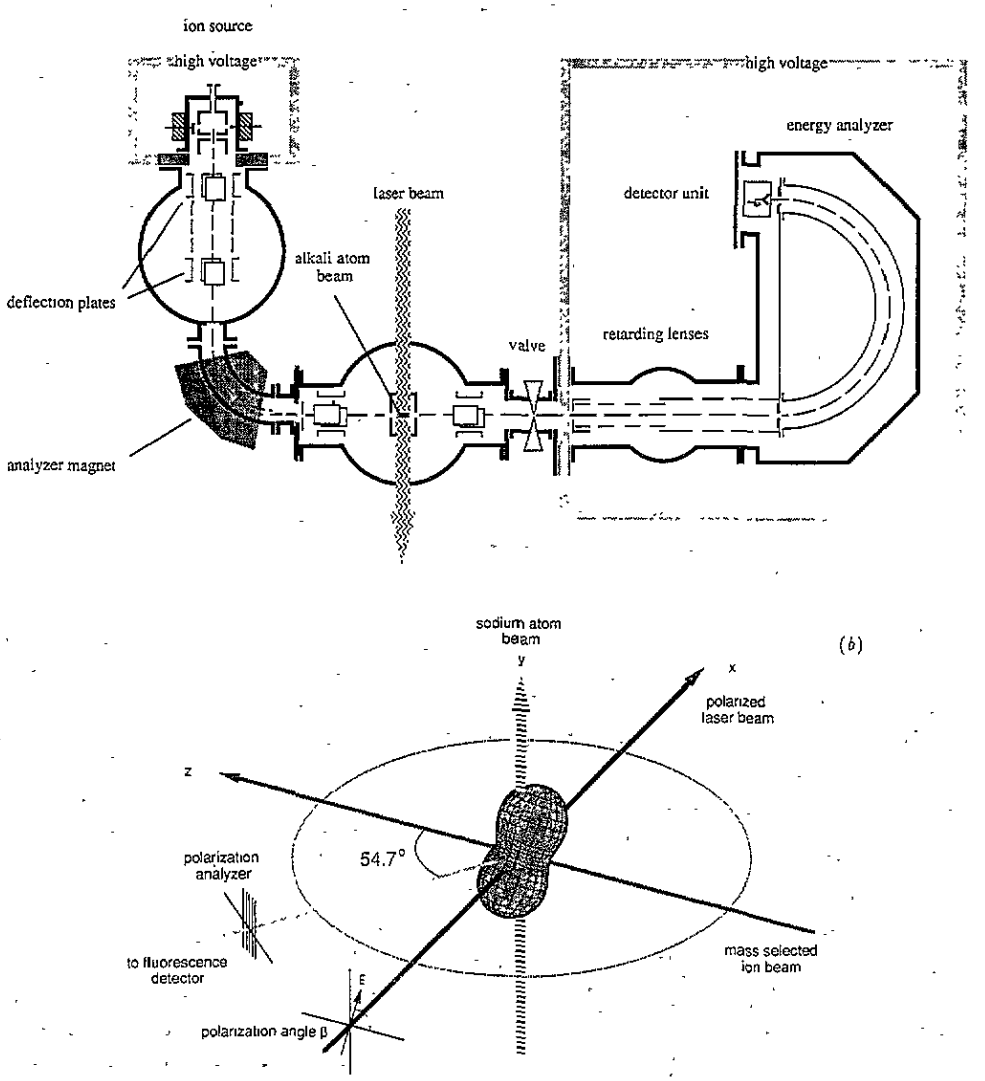

Figure 1. (*a*) Schematic view of the translational energy spectrometer used to study electron capture in collisions of $^4He^{2+}$ with Na(3s) and laser-excited Na*(3p) atoms, respectively. (*b*) Crossed beam reaction geometry, where ion beam, target atom beam and laser beam cross each other under 90°. The shape of the Na*(3p) atom charge cloud as prepared by linearly polarized laser light is indicated. A polarization analyser has been applied to determine the initial state distribution of the magnetic sublevels.

The $^4He^{2+}$ ions have been produced in a Nier-type ion source and were accelerated to 2–12 keV (cf figure 1(*a*)), selected by an analysing magnet and crossed under 90° with a highly collimated Na beam effusing from a double chamber oven (for a more detailed description of this Na beam target cf Gieler *et al* 1991). Charge-exchanged projectile ions were separated from the primary ions by a series of deceleration lenses, and their translational energy spectra (TES) determined by means of a hemispherical energy analyser

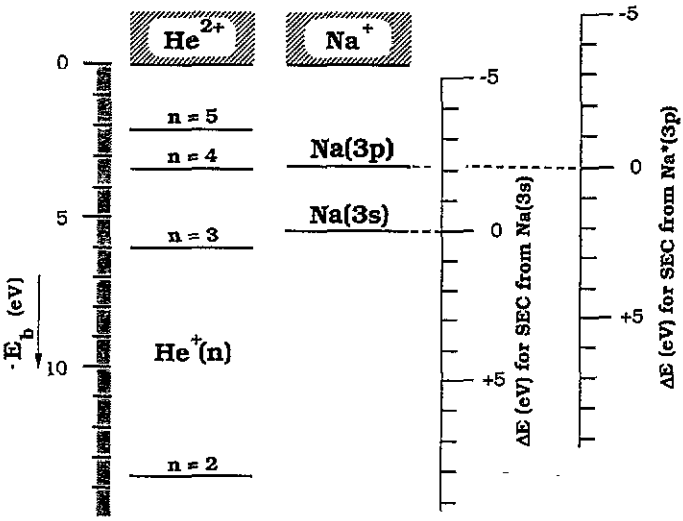

Figure 2. He^+ final-state diagram for electron capture in He^{2+}–Na(3s) and He^{2+}–Na*(3p) collisions, including He II binding energies (E_b) and energy loss/gain scale ΔE for identification of peaks in the translational energy spectra ('SEC' stands for single electron capture).

and a channel electron multiplier. For the TES entrance, a 0.3° FWHM angular acceptance has been determined by placing deflection plates at the position of the target beam and measuring the primary ion beam intensity as a function of deflection angle.

To reduce contributions from He^+ ions formed in collisions with residual gas molecules along the about 1 m long ion flight path, the target region has been enclosed within a small cage (cf figure 1(*a*)) which could be biased at +20 V, thus shifting the translational energy spectrum of charge-exchanged ions in the reaction region with respect to the ones that have captured an electron outside of the cage.

With regard to the laser-excited Na*(3p) target atoms, optical pumping of sodium atoms has been extensively investigated, e.g. by Fischer and Hertel (1982), Meijer (1988), Royer *et al* (1988) and therefore will only briefy be described here.

A tunable, frequency-stabilized CW ring dye laser system (Coherent 699-21) was used to excite the $NaD_2(3^2S_{1/2}\,F = 2 \rightarrow 3^2P_{3/2}\,F = 3)$ transition at 590 nm. Several mirrors directed the chopped laser beam into the interaction chamber where it intersected both the target atom beam and the ion beam under 90° (figure 1(*b*)). A laser beam expander in connection with a 7 mm diameter collimating aperture provided a homogeneous illumination of the sodium target. A laser beam attenuator was used to achieve optimum saturation conditions. Laser light polarization was controlled by a polarizer and a low-voltage modulator (Gsänger LM 0202P5W), permitting a rotation of the linear polarization in the target beam–ion beam plane (figure 2(*b*)). In addition, an electronic device was used to lock the laser to the NaD_2 resonance frequency. The laser frequency was modulated with a few hundred Hz and the resulting fluorescence signal from the Na beam fed into a lock-in amplifier, delivering in this way a correction signal for the external laser frequency control (cf Royer *et al* 1988). By these means the laser could be kept stable for periods of several hours.

Polarization measurements were performed to control the initial population of the magnetic sublevels of the Na*(3p) states. Under ideal pumping conditions a 2:2:5 initial state distribution for the p_x, p_y, p_z substates in the photon reference system can be expected (cf

Fischer and Hertel 1982). A polarization analyser with its transmission oriented in parallel to the atom beam direction in front of a focusing lens and a photo diode were placed in the ion beam–laser beam plane. Assuming the x, y, z orbitals as classical oscillators, simple geometrical considerations show that the photodiode signal directly reflects the 5:2 ratio when the direction of laser polarization is changed from perpendicular to parallel to the ion beam. This arrangement was sufficiently sensitive to show that under our experimental conditions a state distribution of typically 2:2:4.6 could be achieved. Possible reasons for this deviation from the ideal case have been discussed by Fischer and Hertel (1982).

An electronic device was used to control a multichannel analyser accumulating the channeltron signal from the TE spectrometer, the mechanical laser shutter and the low-voltage modulator in such a way that always three TES were subsequently recorded: one TES with laser switched 'off', a second and a third one with laser switched 'on' and laser polarization oriented perpendicular and parallel to the ion beam, respectively. By frequently (about 5 s for each mode) switching between these three measuring modes, an averaging over long term ion and target beam fluctuations could be assured.

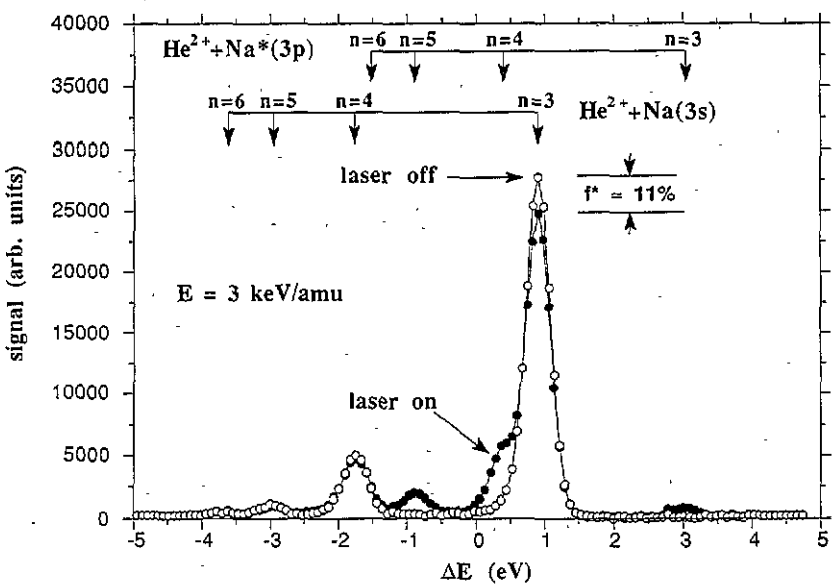

Figure 3. Translational energy spectra for impact of 3 keV amu^{-1} $^4He^{2+}$ on Na. Comparison is made between spectra measured with 'laser on' (full symbols) and 'laser off' (open symbols), respectively. The different final $He^+(n)$ states for capture from respectively Na(3s) and $Na^*(3p)$ have been indicated by arrows. Compared to 'laser off', in the 'laser on' TE spectrum additional peaks occur, whereas the attenuation of the main peak demonstrates the transfer of a fraction f^* of the target atoms into the excited state.

2.2. *TE spectra and data evaluation*

Figure 3 shows typical translational energy spectra (energy resolution $\approx$ 0.4 eV FWHM) for 3 keV amu^{-1} He^{2+} impact on Na, measured with 'laser on' and 'laser off', respectively. For clarity only the 'laser on' spectrum with laser polarization perpendicular to the ion beam direction has been shown. As already known from Schweinzer and Winter (1990), electron

capture from the ground state Na(3s) primarily populates $He^+(n = 3)$ states. Besides this main contribution, capture into $n = 4$ and $n = 5$ can also be identified.

In the spectrum recorded with 'laser on' two effects are apparent (Aumayr *et al* 1991).

- Additional peaks in the TE spectrum arise which can be attributed to capture from $Na^*(3p)$ because of their exothermic energy shift of 2.1 eV with respect to the peak positions in the 'laser off' spectrum.
- The transfer of a fraction of Na target atoms to the excited 3p state manifests itself in an intensity decrease of the peak at $\Delta E = +0.91$ eV corresponding to capture from ground state Na(3s) into $He^+(n = 3)$. This offers a convenient way to determine the fraction f^* of excited $Na^*(3p)$ states in the target atom beam '*in situ*'. As can be seen from figure 3, typically 10% of the sodium atoms could be prepared in the excited state (cf Gieler *et al* 1991, Aumayr *et al* 1991).

Once the fraction f^* is known, 'pure' $Na^*(3p\perp)$ and $Na^*(3p\parallel)$ related TES (S^*) could be obtained by suitable scaling and comparing laser 'on' (S_{on}) with 'off' (S_{off}) spectra.

$$S^* = \frac{1}{f^*}(S_{on} - (1 - f^*)S_{off}) \tag{2}$$

Results for 3 and 0.5 keV amu^{-1} impact energy are presented in figures 4 and 5, respectively. Figures 4(*a*) and 5(*a*) show TES for collisions with ground state Na(3s) atoms, demonstrating the dominance of capture into the $He^+(n = 3)$ state. Figures 4(*b*), (*c*) and 5(*b*), (*c*) display TES for capture from excited Na(3p) atoms with light polarization being parallel (*b*) and perpendicular (*c*) to the primary ion beam direction, respectively.

From the figures it is obvious that the states selected in the electron capture processes from excited $Na^*(3p)$ are dramatically different from those for capture from ground state target atoms. At 3 keV amu^{-1}, capture from $Na^*(3p)$ into $He^+(n = 4)$ and $He^+(n = 5)$ states is strongly enhanced. On the other hand, capture into $He^+(n = 3)$ decreases significantly. This selectivity is still more pronounced for low impact energies, where an almost complete 'switching' from capture into $He^+(n = 3)$ (Na(3s) target) to capture into $He^+(n = 4)$ ($Na^*(3p)$ target) takes place (cf figure 5).

Furthermore, comparison of figures 4(*b*) and 4(*c*) reveals that the probability for capture into $He^+(n = 4)$ decreases if the laser polarization is rotated from perpendicular to parallel to the ion beam direction, while the opposite is found for capture into $He^+(n = 5)$ and $He^+(n = 3)$ final states.

From the TES, apparent relative cross sections $\sigma_{3p\perp}(n)/\sigma_{3s}(n = 3)$ and $\sigma_{3p\parallel}(n)/\sigma_{3s}(n = 3)$ for electron capture from $Na^*(3p)$ into the $He^+(n = 3, 4, 5)$ final states could be derived and compared with those for capture from Na(3s) into the dominant $He^+(n = 3)$ (cf figures 4(*a*) and 5(*a*)) state, by using a least-squares fitting procedure (Schweinzer *et al* 1988, Aumayr *et al* 1989).

The observed polarization dependence of the electron capture process reflects the capture probability depending on the initial alignment of the $Na^*(3p)$ orbital with respect to the projectile direction.

Although it is not possible to prepare pure $3p\Sigma$, $3p\Pi^+$ and $3p\Pi^-$ atomic orbitals (here Σ and Π label the molecular symmetry of the entrance channel in the $R \to \infty$ asymptotic limit consistent with the notation of molecular physics, and the $+/-$ signs refer to the symmetry of orbitals with respect to reflection in the collision plane, cf Dowek *et al* (1990)), a clear relation between cross sections involving Σ and Π orbitals and our measured quantities ($\sigma_{3p\perp}$ and $\sigma_{3p\parallel}$) can be established.

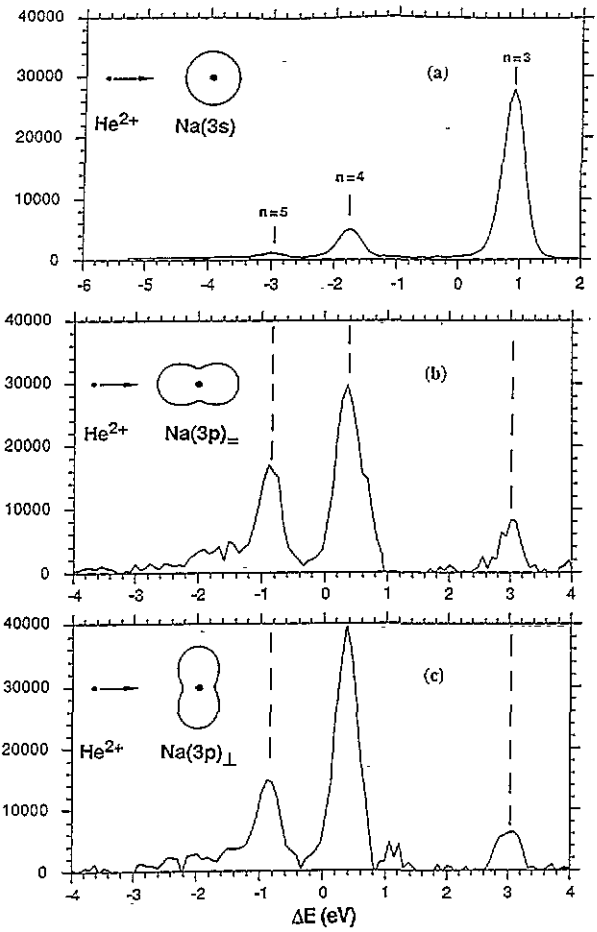

Figure 4. Translational energy spectra for impact of 3 keV amu^{-1} $^4He^{2+}$ on (*a*) Na(3s) (upper panel), (*b*) Na*(3p) with laser light polarization parallel (middle panel) and (*c*) perpendicular (lower panel) to the He^{2+} beam direction, plotted against the reaction energy defect ΔE. The different final $He^+(n)$ states for capture from respectively Na(3s) and Na*(3p) have been indicated by vertical broken lines. In addition, the shape of the Na valence electron charge cloud prior to the collision is illustrated, with laser light incident from a direction perpendicular to the figure plane.

Under ideal pumping conditions these cross sections are interrelated (Royer *et al* 1988) in the following way.

$$\sigma_{3p\parallel}(n) = \tfrac{5}{9}\sigma_{3p\Sigma}(n) + \tfrac{4}{9}\sigma_{3p\Pi}(n)$$
$$\sigma_{3p\perp}(n) = \tfrac{2}{9}\sigma_{3p\Sigma}(n) + \tfrac{7}{9}\sigma_{3p\Pi}(n). \qquad (3)$$

Since in our measurements the collision plane has not been defined, the cross sections for capture from Π^+ and Π^- target states have to be averaged, leading to the cross section $\sigma_{3p\Pi}$. In our case due to the slight deviation from ideal pumping conditions, these linear combinations had to be modified appropriately, and correspondingly apparent experimental cross section ratios $\sigma_{3p\Sigma}(n)/\sigma_{3s}(n=3)$ and $\sigma_{3p\Pi}(n)/\sigma_{3s}(n=3)$ have been obtained.

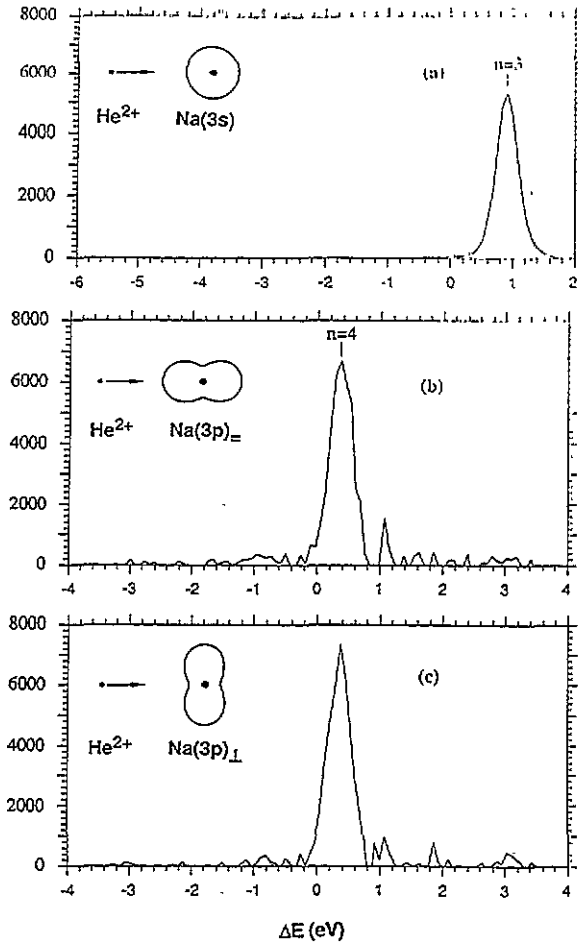

Figure 5. Same as for figure 4, but for 0.5 keV amu^{-1} $^4He^{2+}$ impact energy.

3. AO close-coupling calculations

The semiclassical close-coupling method is a standard approach to describe atomic collision processes (Nielsen *et al* 1990). There, the scattering wavefunction is expanded in eigenstates of the atomic Hamiltonians on both collision centres. The presented collision system is a typical quasi one-electron system where the interaction between the active outer shell electron and the Na^+ core is described by a model potential (Bardsley 1974). We have employed the potential of Rapp and Chang (1973). The corresponding 3s, 3p, 3d states were obtained by diagonalizing the one-centre Schrödinger equation in a truncated Hilbert space of effective-charge hydrogenic states. The radial part of the Na(3s, 3p, 3d) states have been represented by a sum of 3, 2 and 1 effective-charge hydrogenic states, respectively.

Since electron capture is the dominant inelastic reaction channel, expansion of the scattering state must include a large number of travelling orbits centred around the projectile, as well. In this work we have extended this part of the Hilbert space to include the complete $n = 1$ up to $n = 5$ shells on the projectile, getting together with the target-centred states 64 bound states (AO64). Projectile states are given exactly as hydrogen-like $Z = 2$ states.

This basis is now somewhat larger than in our previous work (AO39) (Aumayr *et al* 1992), where the $n = 5$ shell has been excluded. With this basis the time-dependent Schrödinger equation has been solved in a straight-line trajectory approximation for the heavy particle motion,

$$R(t) = b + vt \tag{4}$$

in a space-fixed target centred coordinate frame with quantization axis parallel to the projectile trajectory.

Since this large basis requires considerable CPU time both for evaluation of matrix elements and integration along the trajectory, special properties of the collision system have been utilized.

(i) States with positive and negative reflection symmetry with respect to the collision plane are formed to split the basis into two uncoupled sets of states.

(ii) The calculation for velocity-independent one-centre coupling elements is only performed once for calculating the cross sections for different impact energies.

(iii) In the case of positive reflection symmetry the scattering amplitudes for all relevant initial Na(3s,3p) states are calculated in parallel, based on a single calculation of matrix elements on an appropriate R mesh.

(iv) The non-Hermiticity relation between matrix elements (Green 1965),

$$\mathrm{i}\frac{\mathrm{d}}{\mathrm{d}t}S = M^{\dagger} - M \tag{5}$$

is used to reduce the number of necessary two-centre coupling matrix elements to calculate.

We have found that the system of equations with large basis size becomes increasingly unstable at low impact energies $v < 0.2$, this being due to the fact that the Na wavefunctions are not exact eigenfunctions of the model potential. A calculation of the same basis size with pure hydrogenic wavefunctions on both centres keeps stable even for very low impact energies. For this reason we only present cross sections for impact energies > 1 keV amu^{-1}. Numerical results have been checked by repeating the calculation and exchanging the projectile with the target.

Though experimental results are only provided between 0.5 and 3 keV amu^{-1}, we extended the energy range of our calculation to higher energies, where the AO close coupling description should be more valid. These numerical results are given in table 1 in the impact energy range 1–12 keV amu^{-1}.

4. Results and discussion

In order to compare our experimental results with the calculated ones, the relative experimental cross sections for He^{2+}–Na*(3p) collisions had to be put on an absolute scale by normalization to cross sections for He^{2+}–Na(3s) reactions. In figure 6 the experimental data for total single electron capture (SEC) in He^{2+}–Na(3s) collisions of Schweinzer and Winter (1990) and DuBois and Toburen (1985) are plotted together with the available calculated cross sections of Kumar *et al* (1990) and the results of our calculations. The data reported by Schweinzer and Winter (1990) in the energy range 0.1–1.5 keV amu^{-1} exhibit only a weak impact energy dependence and agree well with the theoretical results. Moreover, the calculations show a flat behaviour in the impact energy dependence of the cross section over

Table 1. Calculated cross sections (in units of 10^{-16} cm^2) for SEC into $He^+(n = 3, 4, 5)$ final states in collisions of He^{2+} with $Na^*(3p\Sigma)$, $Na^*(3p\Pi^+)$ and $Na^*(3p\Pi^-)$, respectively, against ion impact energy.

(a) Initial state $Na^*(3p\Sigma)$

E (keV amu^{-1})	$\sigma_\Sigma(3)$	$\sigma_\Sigma(4)$	$\sigma_\Sigma(5)$
1.0	19	134	45
1.5	29	118	45
2.0	30	78	60
2.5	31	70	72
3.0	34	68	75
4.0	31	69	57
6.0	25	60	39
9.0	14	30	24
12.0	12	19	18

(b) Initial state $Na^*(3p\Pi^+)$

E (keV amu^{-1})	$\sigma_{\Pi^+}(3)$	$\sigma_{\Pi^+}(4)$	$\sigma_{\Pi^+}(5)$
1.0	24	400	40
1.5	21	359	49
2.0	20	308	54
2.5	22	261	57
3.0	21	219	60
4.0	27	153	59
6.0	24	74	47
9.0	13	28	24
12.0	6	11	12

(c) Initial state $Na^*(3p\Pi^-)$

E (keV amu^{-1})	$\sigma_{\Pi^-}(3)$	$\sigma_{\Pi^-}(4)$	$\sigma_{\Pi^-}(5)$
1.0	14	120	6
1.5	20	128	9
2.0	25	128	12
2.5	29	121	13
3.0	31	110	14
4.0	31	92	14
6.0	24	59	18
9.0	12	27	17
12.0	6	12	11

a wide energy range. A constant total SEC cross section of 128×10^{-16} cm^2 has therefore been assumed as a good approximation in the energy range 0.5–3 keV amu^{-1}, and was used for normalization.

In figures 7(*a*) and 7(*b*) such obtained absolute experimental cross sections for capture into $He^+(n = 3, 4, 5)$ from $3p\Sigma$ and $3p\Pi$ initial states are compared with the theoretical results of the AO64 calculation. Table 2 gives the corresponding partial experimental cross sections. Error bars for the experimental data shown in figure 7 and given in table 2 include statistical uncertainties (data reproducibility), errors connected to data evaluation (fitting procedure, energy calibration) as well as errors in the determination of f^* (excited state population) and in the target polarization measurements (cf section 2.2). However, the indicated error bars do not include errors due to the above-mentioned normalization procedure (estimated with ±20%) and errors arising from scattering losses, which are

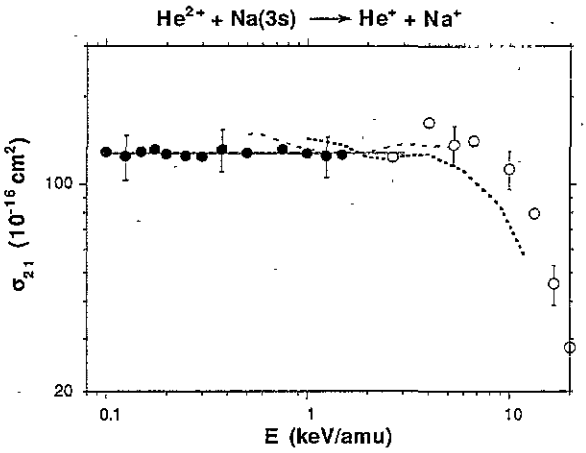

Figure 6. Experimental and calculated cross sections for total SEC in He^{2+}–Na(3s) collisions as a function of impact energy. The straight line (——) indicates the constant value 128×10^{-16} cm^2 used to normalize the experimental cross sections for He^{2+}–$Na^*(3p)$ collisions (cf text). Experimental results: ●, Schweinzer and Winter (1990); ○, DuBois and Toburen 1985. Calculated results: ·····, this work; ----, Kumar *et al* (1990).

probably not important for $He^+(n = 4)$ formation, but possibly for the $He^+(n = 3, 5)$ contributions at low impact energies. A more detailed analysis of the related problems is beyond the scope of this work, since it would require angle-resolved scattering experiments (Jellen-Wutte *et al* 1987).

We also compare results for SEC into $He^+(n = 3, 4)$ from the previous AO39 calculation (Aumayr *et al* 1992) with our new AO64 data (cf figures 7(*a*),(*b*)). SEC from the 3pΠ initial state into $He^+(n = 3, 4)$ is not sensitive to the inclusion of $He^+(n = 5)$ in the AO basis set, as can be deduced from the only small differences found between the results of the AO39 and AO64 calculations (cf figure 7(*b*)), respectively. SEC into different n-shells takes place in a non-competitive way, because including the $n = 5$ shell leads only to an additional flow of probability to these states, without efficiently altering the amplitudes to $n = 3$ and $n = 4$ final states. Experimental and theoretical data are in excellent agreement for SEC into $He^+(n = 3, 4)$, whereas contributions of the $n = 5$ shell to the total SEC process are underestimated in our calculations, especially for higher impact energies. The situation is quite different for the 3pΣ initial state (cf figure 7(*b*)). Results for SEC into $He^+(n = 3, 4)$ are considerably more strongly influenced by inclusion of the $n = 5$ shell. SEC into $He^+(n = 5)$ is strongly competitive with SEC into the $He^+(n = 4)$ shell. This fact can also be deduced from the non-monotonic energy dependency of the total SEC cross section in this energy range.

The agreement of the AO64 results with experimental data is satisfactory except for the $He^+(n = 4)$ contribution. Population of $He^+(n = 4)$ for $E > 2$ keV amu^{-1} is enhanced when including the $n = 5$ shell, and the already present disagreement of the AO39 calculation with the experimental results is becoming even worse (AO64, AO39, cf figure 7(*b*)). The minimum in the partial cross section for population of the $He^+(n = 4)$ shell suggested by our experimental results cannot be reproduced by our present close coupling calculations.

When SEC is not dominated by electron transfer into one single shell, interaction between final states belonging to different shells becomes important. Thus SEC for such a system in the close coupling description is determined by many different matrix elements and their

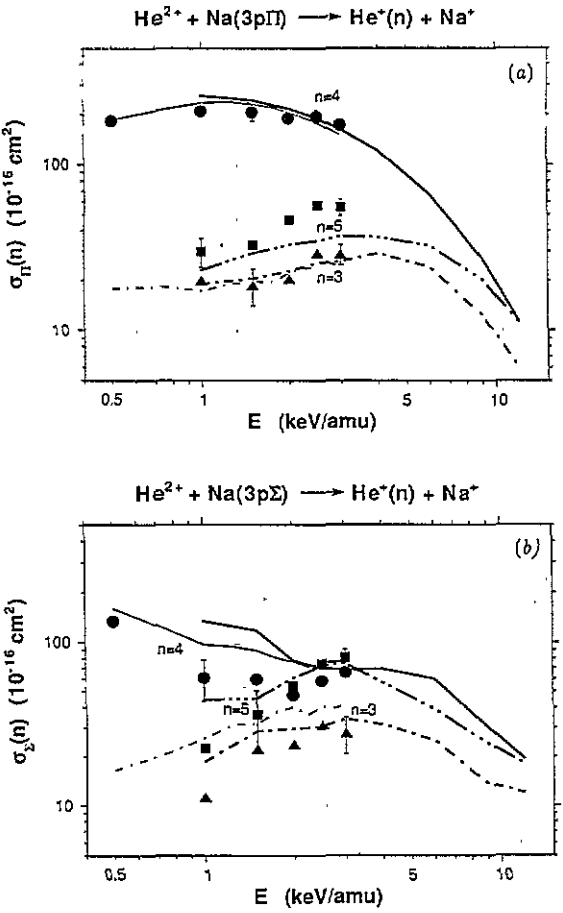

Figure 7. Absolute experimental and calculated data for total and partial SEC cross sections into $He^+(n = 3, 4, 5)$ final states in collisions of $^4He^{2+}$ with (*a*) $Na^*(3p\Pi)$, (*b*) $Na^*(3p\Sigma)$ plotted against ion impact energy. Comparison is made between experimental data (symbols) which have been evaluated from TES obtained with laser light polarization respectively parallel and perpendicular to the ion beam direction, and results of the AO64 calculations of this work (thick lines) and the AO39 calculations of Aumayr *et al* (1992) (thin lines).

		Calculated results	
Experimental results SEC into:		This work AO64	Aumayr *et al* 1992 AO39
$He^+(n = 3)$	▲	— · —	— · —
$He^+(n = 4)$	●	——	——
$He^+(n = 5)$	■	— · · · —	· · ·

complex interrelations, whereas in the case of one dominant shell direct coupling between the initial state and the final principal shell states determines the SEC process to a sufficient extent. Consequently, errors occurring in the model potential, the corresponding states and the incompleteness of the basis have—in the case of competitive channels—an increased influence on close-coupling results especially at low impact energies (cf section 3).

The present calculations and experimental results show that for the 3pΠ initial state

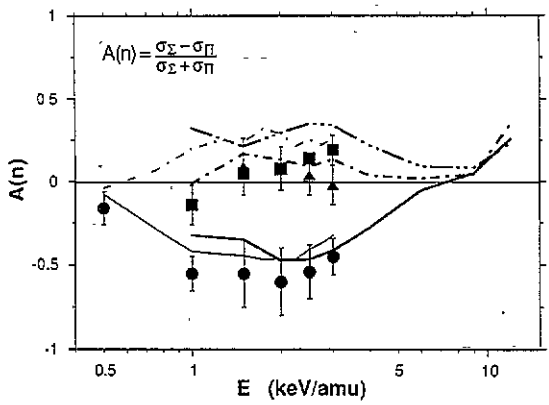

Figure 8. The Σ–Π alignment parameter $A(n)$ for $He^+(n = 3, 4, 5)$ final states plotted against incident $^4He^{2+}$ energy. Experimental data (symbols) are compared with the results of AO calculations (thick and thin lines correspond to AO64 and AO39, respectively).

		Theoretical results	
		This work	Aumayr *et al* 1992
Experimental results		AO64	AO39
$A(3)$	▲	— · —	— · —
$A(4)$	●	——	——
$A(5)$	■	— · · · —	

Table 2. Experimental cross sections (in units of 10^{-16} cm^2) for SEC into $He^+(n = 3, 4, 5)$ final states in collisions of He^{2+} with $Na^*(3p\Sigma)$, and $Na^*(3p\Pi)$, respectively, plotted against ion impact energy. The error bars include neither errors due to the normalization of our results to data for He^{2+}–Na(3s) collisions nor errors due to scattering losses (cf text). The alignment parameters $A(n = 3, 4, 5)$ are also tabulated.

E (keV amu^{-1})	$\sigma_\Sigma(4)$	$\sigma_\Pi(4)$	$\sigma_\Sigma(5)$	$\sigma_\Pi(5)$	$\sigma_\Sigma(3)$	$\sigma_\Pi(3)$
0.5	134 ± 17	184 ± 12				
1.0	61 ± 17	210 ± 12	22 ± 7	30 ± 6		
1.5	60 ± 35	208 ± 25	36 ± 14	33 ± 10	22 ± 6	19 ± 5
2.0	47 ± 30	191 ± 23	54 ± 11	46 ± 8	24 ± 7	20 ± 5
2.5	58 ± 26	195 ± 19	74 ± 13	57 ± 8	31 ± 7	29 ± 5
3.0	66 ± 17	174 ± 13	81 ± 10	56 ± 6	28 ± 7	29 ± 4
E (keV amu^{-1})	$A(4)$	$A(5)$	$A(3)$			
0.5	-0.16 ± 0.07					
1.0	-0.55 ± 0.1	-0.14 ± 0.18				
1.5	-0.55 ± 0.21	0.05 ± 0.25	0.09 ± 0.19			
2.0	-0.60 ± 0.2	0.08 ± 0.13	0.07 ± 0.19			
2.5	-0.54 ± 0.16	0.14 ± 0.11	0.04 ± 0.14			
3.0	-0.45 ± 0.11	0.19 ± 0.08	-0.02 ± 0.14			

larger impact parameters contribute to formation of He^+ ($n = 4$) states than for SEC from $3p\Sigma$ state. This is in agreement with the intuitive geometrical picture of a final state charge cloud resulting in an enhanced overlap with an initial state extending perpendicular to the ion beam direction. However, this simple explanation is certainly not sufficient for coupling mechanisms proceeding at comparable smaller internuclear distances, and therefore has to be taken with some care.

The difference in behaviour of Σ and Π orbitals is usually described by defining an

alignment parameter $A(n)$ with $-1 \leqslant A(n) \leqslant 1$ (Dowek *et al* 1990).

$$A(n) = \frac{\sigma_{3p\Sigma}(n) - \sigma_{3p\Pi}(n)}{\sigma_{3p\Sigma}(n) + \sigma_{3p\Pi}(n)}. \tag{6}$$

The resulting impact energy dependence of this anisotropy parameter has been compared in figure 8 for both our experimental and calculated data. The results of the AO39 calculations of Aumayr *et al* (1992) have also been added.

Apart from the lowest impact energy, capture into $He^+(n = 4)$ from $3p\Pi$ states is almost three times more probable than capture from $3p\Sigma$ states. The situation is different for capture into $He^+(n = 3)$ and $He^+(n = 5)$. Our theoretical curves agree well with the experimental results, except at low impact energies, where discrepancies of $A(4)$ reflect the disagreement in $He^+(n = 4)$ cross sections for capture from $3p\Sigma$ (cf figure 7(*b*)).

When proceeding from the AO39 to the AO64 calculations, a better agreement with experimental data is found for $A(3)$ but not for $A(4)$, as a consequence of the still worse reproduction of the experimental $3p\Sigma$ cross section (cf discussion above). For $A(5)$ the calculations give a similar trend with impact energy as the experimental data, but a considerable deviation becomes obvious at 1 keV amu^{-1}. Finally, a change in the sign for $A(4)$ is predicted by our calculations at an impact energy of about 7 keV amu^{-1}. For higher impact energies the alignment parameter $A(n)$ behaves in a similar way for all presented final principal shells.

In conclusion, absolute experimental cross sections for SEC from Na(3s), Na*(3pΠ) and Na*(3pΣ) initial states into $He^+(n = 3, 4, 5)$ final states by 0.5–3 keV amu^{-1} He^{2+} primary ions have been determined. The experimental results can be satisfactorily reproduced by atomic orbital expansion close coupling calculations including all relevant reaction channels. However, the He^{2+}–Na*(3pΣ) system remains a challenge for future efforts.

A strong effect of the initial target atom alignment for electron capture in collisions with laser-excited Na*(3p) atoms has been found. No general trend in the n-dependent alignment parameter $A(n)$ could be observed at low impact energies. The negative value of $A(4)$ can be explained in a simple picture by the different shape of the inital charge cloud density. At higher impact energies, however, an n-independent behaviour of $A(n)$ is predicted by our calculations, suggesting further experimental work in this energy range.

A more detailed understanding can be expected from angle resolved experiments. In particular, the relation between right/left side collisions in the semiclassical picture in relation to the quantum scattering amplitude suggests a future benchmark experiment to improve the understanding of semiclassical and quantal phenomena.

Acknowledgments

This work has been supported by Fonds zur Förderung der wissenschaftlichen Forschung (Projekt Nr 7006) and by Kommission zur Koordination der Kernfusionsforschung at the Austrian Academy of Sciences.

References

Allan R J, Shingal R and Flower D R 1986 *J. Phys. B: At. Mol. Phys.* **19** L251
Aumayr F, Gieler M, Schweinzer J, Winter H P and Hansen J P 1992 *Phys. Rev. Lett.* **68** 3277
Aumayr F, Gieler M, Unterreiter E and Winter H P 1991 *Europhys. Lett.* **16** 557

Aumayr F, Schweinzer J and Winter H P 1989 *J. Phys. B: At. Mol. Opt. Phys.* **22** 1027
Bähring A, Hertel I V, Meyer E and Schmidt H 1983 *Z. Phys.* A **312** 293
Bardsley J N 1974 *Case Studies At. Phys.* **4** 299
Campbell E E B, Hülser H, Witte R and Hertel I V 1990 *Z. Phys.* D **16** 21
Campbell E E B, Schmidt H and Hertel I V 1988 *Adv. Chem. Phys.* **72** 37
Dowek D, Houver J C, Pommier J, Richter C and Royer T 1990 *Phys. Rev. Lett.* **64** 1713
Driessen J P J, Christopher J S and Leone S R 1991 *Phys. Rev. Lett.* **44** R1421
Dubois A, Nielsen S E and Hansen J P 1993 *J. Phys. B: At. Mol. Opt. Phys.* **26** 705
DuBois R D and Toburen L H 1985 *Phys. Rev.* A **31** 3603
Düren R and Hasselbrink E 1986 *J. Chem. Phys.* **85** 1880
Finck K, Wang Y, Roller-Lutz Z and Lutz H O 1988 *Phys. Rev.* A **38** 6115
Fischer A and Hertel I V 1982 *Z. Phys.* A **304** 103
Gieler M, Hütteneder M, Aumayr F and Winter H P 1991 *J. Phys. B: At. Mol. Opt. Phys.* **24** 4419
Green A T 1965 *Proc. Phys. Soc.* **86** 1017
Hansen J P, Kocbach L, Dubois A and Nielsen S E 1990 *Phys. Rev. Lett.* **64** 2491
Hansen J P, Nielsen S E and Dubois A 1992 *Phys. Rev.* A **46** 5331
Hertel I V and Stoll W 1974 *J. Phys. B: At. Mol. Phys.* **7** 570
—— 1978 *Adv. At. Mol. Phys.* **13** 113
Houver J C, Dowek D, Richter C and Andersen N 1992 *Phys. Rev. Lett.* **68** 162
Jellen-Wutte U, Schweinzer J, Krammer M and Winter H 1987 *Nucl. Instrum. Methods* B **23** 59
Kumar A, Lane N F and Kimura M 1990 *Phys. Rev.* A **42** 3861
Meijer H A J 1988 *Theses* University of Utrecht, The Netherlands
Meijer H A J, van der Meulen H P and Morgenstern R 1987 *Z. Phys.* D **5** 299
Nielsen S E, Hansen J P and Dubois A 1990 *J. Phys. B: At. Mol. Opt. Phys.* **23** 2595
Rapp D and Chang C 1973 *J. Chem. Phys.* **58** 2657
Richter C, Andersen N, Brenot J C, Dowek D, Houver J C, Salgado J and Thomsen J W 1993 *J. Phys. B: At. Mol. Opt. Phys.* **26** 723
Roncin P, Adjouri C, Gaboriaud M N, Guillemot L, Barat M and Andersen N 1990 *Phys. Rev. Lett.* **65** 3261
Royer T, Dowek D, Houver J C, Pommier J and Andersen N 1988 *Z. Phys.* D **10** 45
Schweinzer J, Jellen-Wutte U, Vanek W, Winter H and Hansen J E 1988 *J. Phys. B: At. Mol. Opt. Phys.* **21** 315
Schweinzer J and Winter H P 1990 *J. Phys. B: At. Mol. Opt. Phys.* **23** 3881
Witte R, Campbell E E B, Richter C, Schmid H and Hertel I V 1987 *Z. Phys.* D **5** 101